Heritage Science

RESEARCH

Open Access

Dynamically documenting archaeological excavations based on 3D modeling: a case study of the excavation of the #3 fossil of hominin cranium from *Yunxian*, Hubei, China

Wenyuan Niu[1,2,4,6,7,9†], Chengqiu Lu[3†], Qiushi Zou[1,6,7], Yunbing Luo[3], Xuan Wang[4], Hanyu Xiang[4], Fan Zhang[1,4,7,9], Xing Gao[5], Song Xing[5], Xuan Wei[1,6], Wentai Lou[1,6,10], Dailong Huang[9], Cheng Wang[9], Dongqing Jiang[9], Xiaofeng Wan[11], Zhongyun Zhang[3], Huanghao Yin[3], Jiayang Lu[3], Feng Wang[1,6], Xianfeng Huang[1,4,7,9*] and Yinghua Li[1,6,7,8*]

Abstract

Documenting tangible cultural heritage using 3D modeling techniques is gradually becoming an indispensable component of archaeological practice. The 3D modeling techniques based on photogrammetry and LiDAR scanning enable high-accuracy and high-realistic reconstruction of archaeological sites, and have been proven a powerful tool for documenting archaeological excavations. However, dynamically documenting an ongoing excavation using these techniques is still considered tedious, time-consuming, expensive, and dependent on expertise. Moreover, the application of 3D modeling techniques in archaeological excavations still faces some technical challenges, such as modeling with multi-source and multi-scale data, fusing local models at different times into a whole, achieving fast modeling while GPU workstations are not available in the field, and evaluating the quality of 3D models. As a result, there are still very few archaeological teams deeply engaged in dynamic documentation with 3D modeling techniques, and traditional drawing sketches and taking photographs still dominate. In these senses, documenting the archaeological excavation at the *Yunxian Man* site (located in Hubei, China) is an invaluable opportunity for exploration and practice. Archaeologists determined to conduct dynamically documenting at the beginning of the 6th excavation project for the site, and established a rotation system to reconcile physical excavation with digital preservation. Through repeated practice and communication, we proposed a workflow and pursued several new methods to enhance the feasibility of dynamically documenting, and obtained 4D models of the ongoing archaeological excavations. In 2022, the *Yunxian Man* site unearthed the most intact fossil of hominin cranium from about one million years ago in the Eurasian continent, preserving important and scarce anatomical features of early humans in Asia. As the original taphonomic context of the fossil corroded away during physical excavations, the digital documentation consisting of 4D models serves as permanent original data source in subsequent archaeological research. Moreover, we obtained cross-scale 3D models from geographical environment to archaeological site, excavation area,

[†]Wenyuan Niu and Chengqiu Lu have contributed equally to this work.

*Correspondence:
Xianfeng Huang
hwangxf@gmail.com
Yinghua Li
lyhfrance2005@yahoo.fr
Full list of author information is available at the end of the article

and cultural remains, and all of these 3D models are in an actual, unified coordinate framework. Thus, we can contribute to multidisciplinary cross-collaborative research through data sharing. Considering that digital documentations serve a great value in archaeological research, this paper focuses on sharing the workflow and methods to facilitate digital preservation for more archaeological projects.

Keywords Dynamically documenting, 3D modeling, Multi-source data fusion, The *Yunxian Man* site, Cloud-based modeling, Mesh update, Archaeological excavation, Paleolithic site

Introduction

The irreversible nature and inevitable destructiveness of archaeological excavations make archaeologists place much importance on documenting and archiving. The 3D modeling techniques enable us to document high-accuracy and high-realistic 3D models for archaeological excavations. Performing multiple 3D modeling to document various momentary states of the excavation area can be formulated as dynamically documenting. Dynamically documenting enables comprehensive recording the occurrence and taphonomic context of the archaeological sites in their original stratigraphy and can provide a wealth of details for post-excavation research. As the original taphonomic context corroded away during physical excavations, the digital documentation serves as a permanent 3D data source. This data source supports unlimited observations, measurements, inferential analyses, and multidisciplinary and multi-institutional collaborative research through data sharing.

A brief review of the application of 3D techniques in archaeology and cultural heritage.

In the last 20 years, the application of 3D techniques in archaeology and cultural heritage studies has increased exponentially and has become very common in archaeological practice and cultural heritage conservation. Laser scanning and photogrammetric reconstruction are widely used 3D modeling techniques by archaeologists. Due to the ability to obtain high-precision geometric structures on the surface of objects, laser scanning is used for the protecting and documenting of cultural heritage [1], structural deformation monitoring [2], archaeological excavation documenting [3, 4], etc. Due to the ability to obtain both high-precision geometric structures and highly realistic textures, photogrammetric reconstruction techniques are widely used for small cultural relics [5], historical buildings [6–9], archaeological sites [9–12], and archaeological excavations [13–15]. Some studies have combined laser scanning and photogrammetric reconstruction techniques [16–19]. The abundance of excellent work leads scholars to review the contribution of 3D technology to archaeology and cultural heritage with much praise and more expectations [19–22].

However, we found in our research that there are not many cases of 3D modeling techniques applied to dynamically documenting archaeological excavation. It may be said that the number of archaeological projects with dynamically documenting of 3D modeling techniques is not proportional to the expectations of archaeologists [13, 20, 21]. Some researchers think the main reason is the lack of a straightforward method that can be flexibly and holistically integrated into the complete workflow of archaeological excavations [20]. Some researchers also believe that the efficient integration of 3D technology into daily field work requires a deeper understanding of the technology and some excellent examples [21].

Difficulties in implementing dynamically documenting archaeological excavations and our solutions.

In practice, some reasons and difficulties prevent archaeological teams from flexibly and dynamically applying 3D modeling techniques. These include but are not limited to: (1) There is difficulty in handling and integrating data from millimeter to kilometer scales (cross-scale) and captured by different devices (multi-source). (2) The 3D modeling process is time-consuming and sometimes interferes with fieldwork progress. (3) The highly dynamic process of the excavation makes frequent requirements of 3D modeling and then amplifies the former difficulties. (4) 3D modeling is usually considered indispensable to special equipment for data collection, complex software, and expensive GPU workstations for data processing, and it is especially indispensable to specialized technicians. (5) The varying quality of 3D model data makes archaeologists uneasy.

We consider these practical difficulties in a complete archaeological excavation and solve them with a proposed workflow and several new methods. (1) We deploy a multi-level control network and propose a strategy for fusing cross-scale and multi-source data. (2) We introduce fast cloud-based modeling technology to reduce the time spent on data processing, and solve the dilemma of efficiency requirements and budget shortages. (3) We propose a 4D model fusion method that only needs to focus on the sub-area that is being excavated, thus reducing the workload due to frequent modeling. (4) Together with spatial precision, our novel geometric refinement and texture resolution metrics provide a comprehensive measure of the quality of 3D models. (5) Our

self-developed software is designed to be as simple and concise as possible, making our workflow and methods easy to implement and generalize.

The 6th excavation of the Yunxian Man site—our hands-on opportunity.

The *Yunxian Man* site , also known as the *XuetangLiangzi* site, is located in the village of Mituosi in the Yunyang District (formerly "*Yunxian*") of Shiyan City, Hubei Province, China (Fig. 1). It is about 10 km from Qingqu Town and about 40 km down the Han River to the urban area of Yunyang [23]. The Quyuan River flows from north to south and merges into the Han River. XuetangLiangzi is an east–west gondola, the main body of which is the fourth alluvial terrace on the north bank of the Han River, the top of which is about 50 m above the water surface of the Han River. The site preserves an area of about 1.9 million square meters, with quaternary accumulations of more than 8 m and locally more than 18 m, preserving stratigraphic deposits from different periods over more than 1 million years [24].

Five seasons of excavations between 1989 and 2007 revealed two complete skulls of Homo erectus and a large number of animal fossils and stone artifacts, which attracted great attention from the academic community [23, 25–28]. Combining various geological dating methods, the layer yielding the skull of *Homo erectus* was dated to between 1.1 ± 0.16 Ma and 0.581 ± 0.093 Ma [29, 30].

In 2021, the site was excavated for the 6th season with three excavation areas (the *Excavation Area B, C, E* in Fig. 2). In 2022, the #3 hominin cranium and a large number of animal fossils and lithic artifacts were found in the calcareous cemented sand stratum. A new round of interdisciplinary research on hominin fossils, archaeological remains, site formation process, and absolute dating using multiple methods is underway [24].

The *Yunxian Man* site serves as an excellent opportunity for practicing the concept of dynamically documenting, benefiting from two advantages. Firstly, the site is located in an open and wide location, which makes it easy to fly UAVs and provides adequate light to implement the photogrammetry. Secondly, the archaeologists meticulously planned and organized the 6th excavation of the site, invited the digital preservation team to participate in the fieldwork from the beginning, and communicated repeatedly on the implementation issues of obtaining high-quality digital documentation.

As a result, we propose a workflow and pursue several new methods to practice dynamically documenting archaeological excavation. In this paper, we present

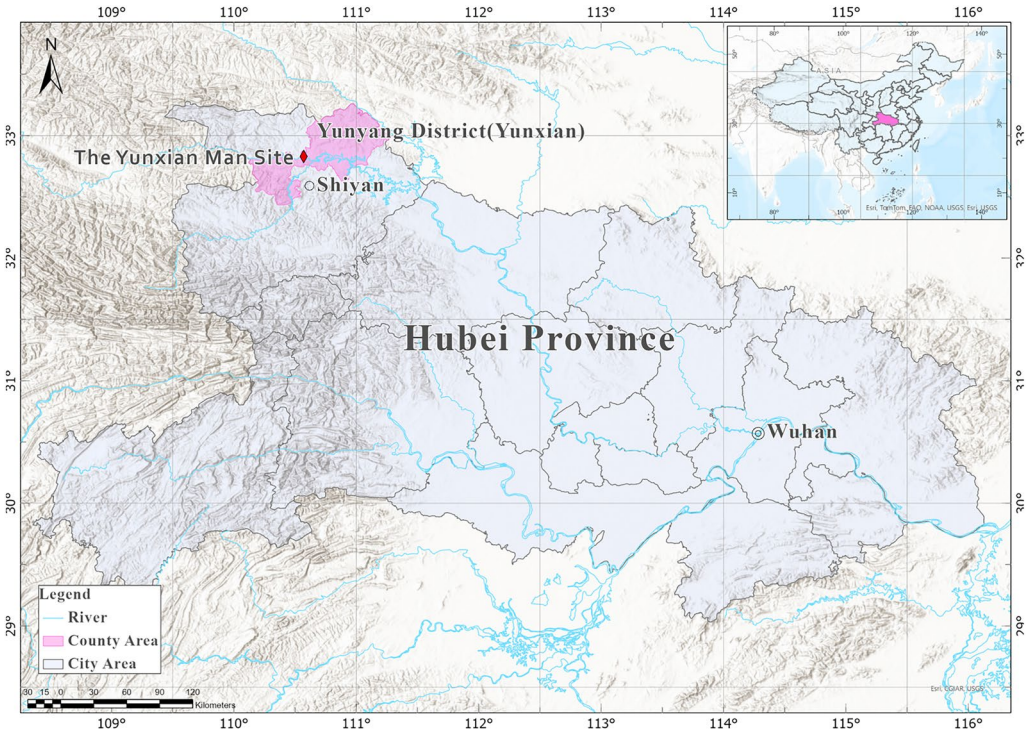

Fig. 1 The location of the *Yunxian Man* site. The site is located in the village of Mituosi in the Yunyang District (formerly "*Yunxian*") of Shiyan City, Hubei Province, China. The first hominin fossil found in 1989 was named *Yunxian Man*, the site was named the *Yunxian Man* site, and these archaeological names are followed to the present day

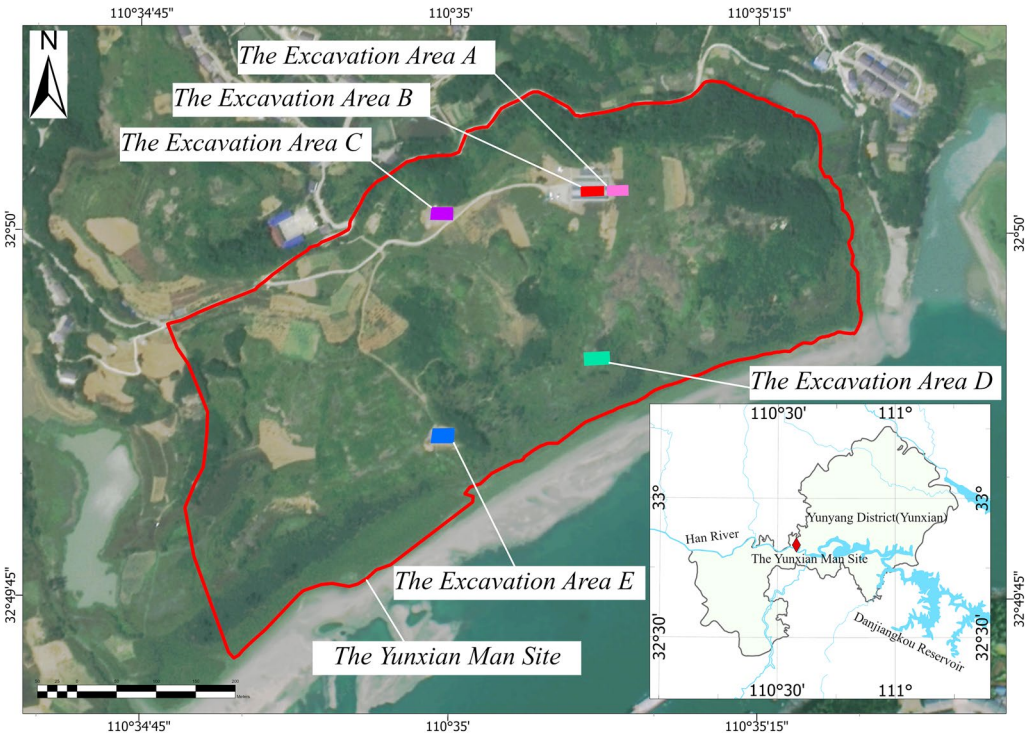

Fig. 2 The location of the excavation area. In 2021, the *Yunxian Man* site launched its 6th season of excavation and defined three excavation areas: the *Excavation Area B*, the *Excavation Area C*, and the *Excavation Area E*

the methods, implementation details, and major results. The self-developed software used in this paper, including GET3D, DasEarth, DasMesh, and DasViewer, can be acquired uniformly from the project homepage (https://wyniu.github.io/DDAE/), or from the product pages referenced in subsequent sections. Readers could contact the authors to get a free license for academic research and cultural heritage preservation purposes. In addition, we will continuously update the project homepage to provide some more data, scripts, tutorials and demo videos to help readers reproduce and promote the methods in this paper.

Materials and methods

To achieve dynamically documenting archaeological excavations practically, we develop a workflow and pursue several new methods. As shown in Fig. 3, the workflow is based on a multi-level control network and consists of five layers:

(1) *Multi-level Control Network:* Constructing a multi-level control network to place cross-scale archaeological objects into an actual and unified coordinate framework.
(2) *Data Collection:* Combining multiple methods to collect original data.
(3) *Data Processing:* Getting 3D models from the original data.
(4) *Data Evaluating:* Quantitatively evaluating the quality of the 3D models.
(5) *Data Application:* Constructing a 4D model database, generating other digital products, and supporting comprehensive analysis and dynamic exhibition.

We apply our workflow and new methods to the excavation of the #3 fossil of hominin cranium from *Yunxian*. Our work involves some key techniques and their necessary equipment and software, we present them in Table 1.

Theoretically, the layer of data application in this workflow belongs to the phase of after excavation. As we focus on how to perform data collection and 3D modeling, and our practice archaeological site—the *Yunxian Man* site is currently in the phase of during excavation, we mainly describe the key methods and techniques in the former four layers in this paper.

Multi-level control network

In general photogrammetric 3D reconstruction projects, GCPs (Ground Control Points) are often used to enable 3D models and 4D products (DOM, Digital Orthophoto Map; DEM, Digital Elevation Model; DRG, Digital Raster

Table 1 The key techniques and their necessary equipment and software

Step	Task	Equipment/software	Our tools[a]	Sections
Multi-level control network	Outdoor survey	RTK (Real Time Kinematic)	Daspatial miniRTK	"Multi-level control network"
	Indoor survey	ETS (Electronic Total Station)	THINRAD TTS-112R10M	
Data collection	Aerial photogrammetry	UAV (Unmanned Aerial Vehicle)	DJI M300	"Data collection"
		Multi-lens camera	Daspatial Shuangyu 7× Pro	
	Close-range photogrammetry	Camera	Canon 5D Mark IV	
	Terrestrial laser scanning	Terrestrial laser scanner	Trimble ×7	
	Portable laser scanning	Portable laser scanner	KScan-Magic II	
Data processing	3D modeling (GPU-required)	Individual or clustered 3D reconstruction software	Daspatial GET3D (Link)	"Multi-source data fusion 3D modeling"
	3D modeling (GPU-free)	Cloud based 3D reconstruction software	Daspatial DasEarth (Link)	"Fast cloud-based 3D modeling"
	3D model post-processing	3D model post-processing software	Daspatial DasMesh (Link)	"4D model fusion"
	Evaluation of 3D data quality	3D model viewer and quality control software	Daspatial DasViewer (Link)	"Evaluation metrics"

[a] To enable readers to reproduce the methods of this paper at their sites, we provide links to all of the software

Graphic; DLG, Digital Line Graphic) to carry geographic coordinates. Before data acquisition, GCPs are deployed in the field, and their geographic coordinates are surveyed. It is necessary to ensure that GCPs are properly sized so that they are visible in the subsequently captured images. By stabbing the surveyed coordinates of the GCPs into the images, 3D models and 4D products can be assigned geographic coordinates.

In archaeological excavation, study objects are cross-scale, as small as millimeters or as large as kilometers. Therefore, it is infeasible to deploy one set of GCPs to fulfill the requirements of being visible in different-scale images or 3D models. To place cross-scale archaeological objects into an actual and unified coordinate framework, we propose a multi-level control network.

The multi-level control network is comprised of different levels and different styles of GCPs, each level visible in the images at a corresponding scale. Tailored for archaeological excavation, we divide the multi-level control network into four levels, Level 1, Level 2, Level 3, and Level 4. The measurement objects applicable to Level 1 to Level 4 sequentially are geographical environment (kilometer level), archaeological site (hundred-meter level), excavation area (meter level), and cultural remains (millimeter level).

Deploying the multi-level control network follows the principle:

(1) While setting up the GCPs as uniformly as possible, we should consider the topography and the importance of the local area;
(2) The GCPs in Level 1 and Level 2 should be kept as stable as possible;
(3) The GCPs in Level 3 and Level 4 should be partly stable and partly dynamically adjusted according to the excavation.

The main equipment used to set up a multi-level control network includes RTK (Real Time Kinematic) and ETS (Electronic Total Station). RTK is used to survey the geographic coordinates of GCPs in areas where CORS (Continuously Operating Reference System) signals are available (usually open outdoor areas). ETS is able to survey geographic coordinates without a CORS signal (usually used indoors), but it requires setting up a station at a point location with known geographic coordinates. We use Daspatial miniRTK and THINRAD TTS-112R10M ETS in our practice.

Data collection

We mainly employ four different methods for data collection (Fig. 4).

(1) *Aerial photogrammetry* is mainly accomplished by a UAV carrying a multi-lens camera. The purpose of this method is to efficiently acquire oblique images for a large-scale scene, which is the necessary input data for 3D modeling. This work requires a trained UAV pilot. After setting the appropriate parameters, the camera works automatically with the UAV's flight. In practice, we use a DJI M300 UAV carrying a self-developed multi-lens camera named

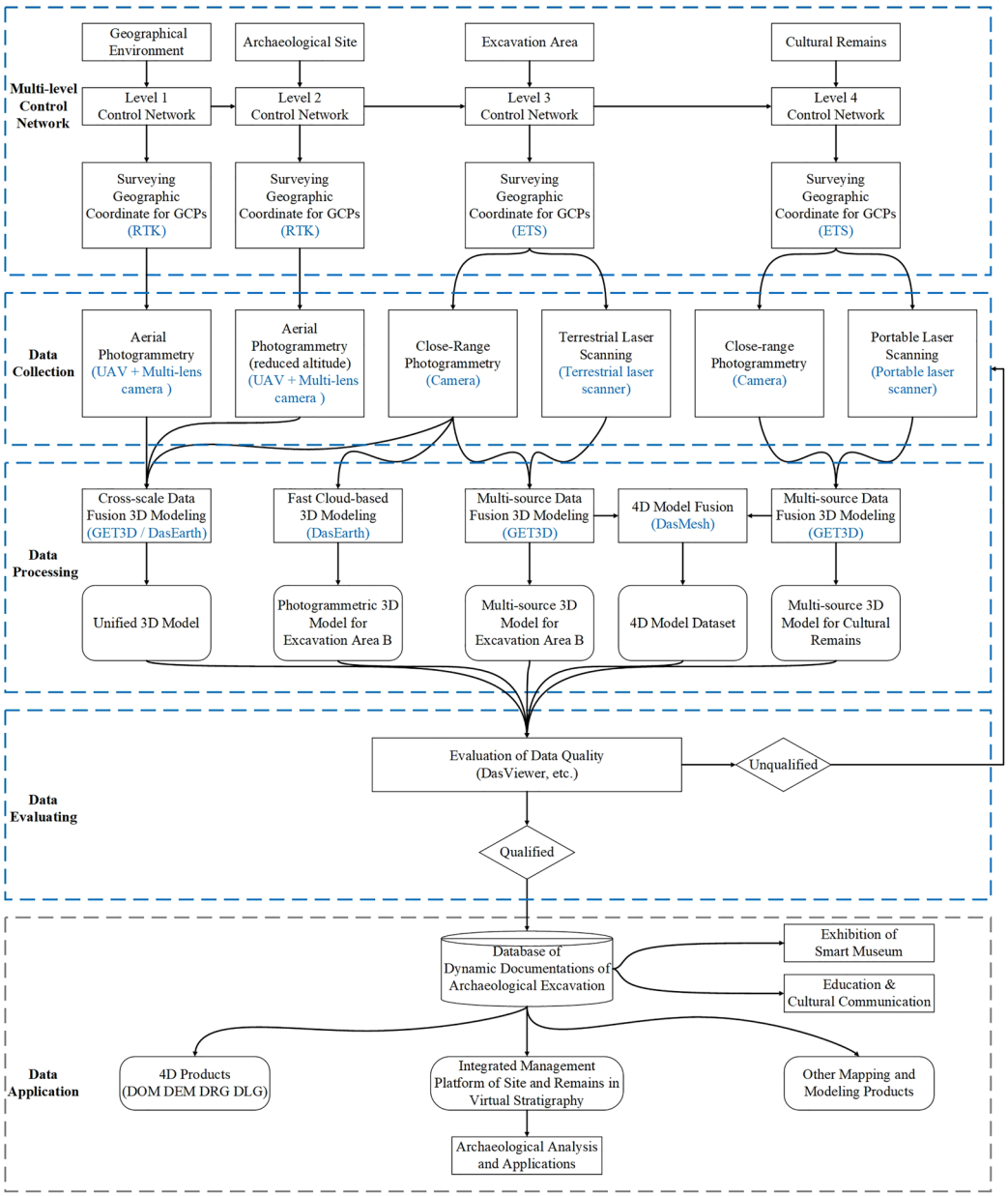

Fig. 3 The workflow of dynamically documenting archaeological excavations. The workflow is based on a multi-level control network and consists of five layers. This paper focuses on the former four layers

Daspatial Shuangyu 7X Pro to accomplish this work.

(2) *Close-range photogrammetry* is mainly accomplished by a camera. The purpose of this method is to acquire close-range images for medium-scale or small-scale scenes. Since this method requires manually taking a large number of photographs, it is usually used for areas where UAVs cannot be maneuvered. With the improvement of our algorithms, this method is not restricted to the type of camera. Whether it is a DSLR camera or a phone camera, we just need to make sure that the images are sufficient in terms of definition and overlap. In practice, we use a Canon 5D Mark IV DSLR camera to accomplish this work.

(3) *Terrestrial laser scanning* is mainly accomplished by a terrestrial laser scanner. The purpose of this method is to acquire laser-scanned point clouds

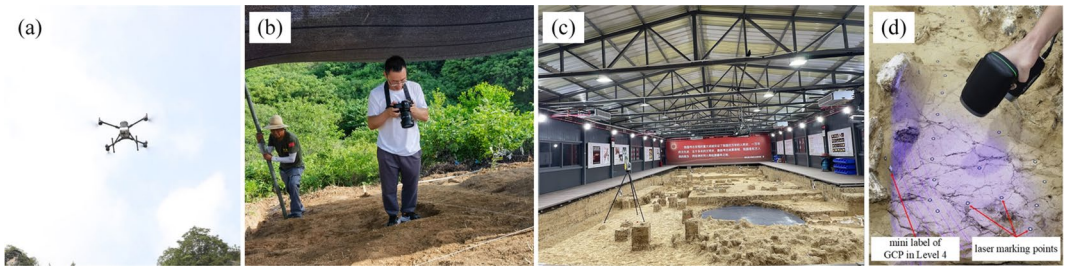

Fig. 4 Data collection methods. **a** Data collection through aerial photogrammetry. **b** Data collection through close-range photogrammetry. **c** Data collection through terrestrial laser scanning. **d** Data collection through portable laser scanning

for medium-scale scenes, which generally provide more accurate geometric information than close-range images. After setting up the scanner in a suitable location and emptying all moving people and objects, we can remotely control the device to start scanning. In practice, we use a Trimble ×7 terrestrial laser scanner to accomplish this work.

(4) *Portable laser scanning* is mainly accomplished by a portable laser scanner coupled with a graphic workstation. The purpose of this method is to acquire a close-range point cloud for small-scale scenes, which is promising to provide the highest accuracy point cloud from the currently available techniques. This method is relatively inefficient due to the demand for affixing many laser marking points and the demand for repeated scanning and inspection. Therefore, we use this method only on significant cultural remains that require sub-millimeter scanning. In practice, we use a KScan-Magic II portable laser scanner to accomplish this work.

Cross-scale data fusion 3D modeling

With the constraints of a cross-scale data fusion algorithm and the multi-level control network, we can make the cross-scale data in an actual and unified coordinate framework. Our cross-scale data fusion algorithm focuses on fusing cross-scale data and constructing a unified 3D model through the following steps:

(1) Automatically group the cross-scale data into several clusters according to the differences in camera parameters.
(2) Separately execute dense matching to obtain a point cloud for each cluster.
(3) Perform adjustments within the cluster to optimize the point cloud, then obtain a high-precision point cloud for each cluster.
(4) Stabbing GCPs of multi-level control network to make the point cloud of each cluster in the actual and unified coordinate frame.
(5) Taking the point clouds of small-scale clusters as a benchmark to gradually fine-tune the scales of point clouds of other clusters, then obtain a cross-scale fused point cloud.
(6) Execute Delaunay triangulation on the cross-scale fused point cloud to construct the geometric model.
(7) Map textures for the geometric model using images. Note that images from small-scale clusters should be prioritized in areas of cross-scale overlapping.

In practice, we perform the above-mentioned operations with GET3D. As a self-developed software, we embed the cross-scale data fusion algorithm into the 3D modeling workflow. Constructing 3D models from cross-scale data with GET3D takes only 4 steps:

(a) *Data importing.* Use the "Import Default Photos" button to import aerial images and the "Import Ground Photos" button to import photos taken with a DSLR camera or smartphone. After clicking the "Confirm" button, the software will automatically complete the above Step 1.
(b) *ATS-free.* Click the "Submit Aerial Triangulation" button and select the "Free Network" mode in the pop-up window. After clicking the Confirm button, the software will automatically complete the above Step 2 and Step 3. These steps mainly employ the photogrammetric technique of aerial triangulation surveying with free network mode, thus abbreviated as ATS-free.
(c) *ATS-control.* After the previous step is finished, use the "edit GCP" button to stab the GCPs of the multi-level control network, then click the "Submit Aerial Triangulation" button and select the "Control Network" mode in the pop-up window. After clicking the Confirm button, the software will complete the above Step 4 and Step 5. These steps mainly employ the photogrammetric technique of aerial triangulation surveying with control network mode, thus abbreviated as ATS-control.

(d) *Producing a 3D model.* After the previous step is finished, click the "Submit Reconstruction" button to start generating 3D models, the software will complete the above Step 6 and Step 7.

After the program finishes running, we can get a cross-scale fused 3D model. Click the "View Product" button, then GET3D (Link) will automatically call the 3D model viewer DasViewer to display the model. After the program finishes running, we can get a cross-scale fused 3D model. Click the "View Product" button, then GET3D will automatically call the 3D model viewer DasViewer to display the model. Generally, GET3D concurrently saves 3D models in OBJ and OSGB file formats. OBJ is easier to edit, and OSGB is easier to load and browse quickly.

Multi-source data fusion 3D modeling

As photogrammetry and LiDAR scanning both offer their own advantages and disadvantages, we usually use the two methods simultaneously to complement each other for excavation areas and cultural remains. To improve on the two methods, we use the a multi-source data fusion algorithm to fuse their data. The algorithm contains the following steps:

(1) Orient and scale the laser-scanned point cloud to assign it actual scale and geographic coordinates.
(2) Execute ATS-free using photogrammetric images to obtain dense point cloud, and then stab GCPs and execute ATS-control to assign it actual scale and geographic coordinates.
(3) Fuse laser-scanned point cloud and dense point cloud into a composite point cloud through ICP (Iterative Closest Point) alignment algorithm [31–33]. The priority of the ICP alignment reference is in the following order: terrestrial laser-scanned point clouds, portable laser-scanned point clouds, and image-matched point clouds. Next, only portable laser-scanned point clouds are retained in the fused point cloud; if there are no portable laser-scanned point clouds, the fused point cloud is processed with outlier noise rejection and uniform downsampling.
(4) Execute Delaunay triangulation on the composite point cloud to construct the geometric model.
(5) Map textures for the geometric model using photogrammetric images.

In practice, we perform the above-mentioned operations with GET3D. As a self-developed software, we embed the multi-source data fusion algorithms into the 3D modeling workflow. Constructing a multi-source fused 3D model using GET3D is similar to a cross-scale fused 3D model, which also includes four steps: data importing, ATS-free, ATS-control, and producing a 3D model. The difference is that when importing data, it is also required to use the "Import Ground LiDAR Point Cloud" button or the "Import Mobile LiDAR Point Cloud" button to import a laser point cloud.

Fast cloud-based 3D modeling

Typically, generating 3D models using images and point clouds is computility-intensive and time-consuming. In the process of dynamically documenting archaeological excavation, it is inevitable to encounter phased surges of modeling demand. To get rid of the restriction of GPUs (which is usually limited by the funding budget) and to cope with the urgent modeling tasks, we adopt the fast cloud-based modeling technique.

The fast cloud-based modeling technique requires computers in 3 roles, including a data server, a host server, and several GPU laborers. Its workflow mainly consists of the following steps:

(1) The user uploads the modeling data to the data server.
(2) The host server divides the modeling task into many similar sub-tasks and dynamically organizes and manages these sub-tasks.
(3) Dispatch the required or available number of GPU laborers.
(4) Each GPU laborer parallelly runs the following tasks in a loop until all sub-tasks are completed:

- fetching a sub-task from the host server,
- fetching the data required for the sub-task from the data server,
- executing the sub-task and getting the result data,
- sending the result data to the host.

Theoretically, only a small part of the procedure in modeling tasks is indivisible. Therefore, most modeling tasks can be chunked, parallelized, and then executed quickly. Our team has developed the fast cloud-based modeling technology as *DasEarth* (Link), an online modeling platform that is open to the public. To perform 3D modeling with DasEarth, all we need to do is upload data and stab GCPs, and then the system will automatically generate a 3D model.

4D model fusion

In archaeological practice, an excavation area is usually divided into several excavation sub-areas. Each excavation sub-area is different in the excavation progress, resulting in different frequencies and dates for modeling. To facilitate unified management and application,

archaeologists need to integrate the 3D models of these scattered excavation sub-areas in different time series into an overall 3D model of the excavation area. The fusion of models from different times into one overall model can be viewed as the addition of a time dimension to a 3D model, so it is also called a 4D model.

To cope with this demand, we propose a method of 4D model fusion. This method enables editing 3D model as if it was a piece of cake, as we can cut away a patch and replace it with a new one. Given that the patch P_{old} that needs to be cut away is on the old 3D model M_{old}, and the patch P_{new} that needs to be made up is on the new 3D model M_{new}, our method constructs an updated 3D model M_{update} through the following steps (Fig. 5):

(1) *Parameter transformation.* Selecting a set of corresponding points $V\{(v_{o1}, v_{n1}), (v_{o2}, v_{n2}), ..., (v_{oi}, v_{ni})\}$ on M_{old} and M_{new} (DasViewer → Measuring → Coordinates Measuring). Using V to calculate the rotation, translation, and scaling parameters, and applying these parameters to M_{new} and make sure that M_{new} coincide with M_{old} (DasMesh → OBJ/OSGB Coordinate Transformation → 7 Parameter Transformation).
(2) *Specifying the update range.* Manually sketch an updated range R (DasViewer → Marking → Add Line → Save as KML).
(3) *Cutting the patching.* Use R to cut the M_{old} and M_{new}, the part of M_{old} outside R named P_{out}, the part of M_{new} within the R named P_{in}. Combine P_{out} and P_{in} as M_{update} (DasMesh → OBJ/OSGB cropping).
(4) *Topological re-connection.* Re-connect the topology of the vertices at the edge of R, so that the P_{out} and P_{in} are truly fused into M_{update} (DasMesh → Model Fusion).
(5) *Texture re-mapping.* Re-map the texture of the triangles at the edge of R, so that the texture align with geometric model (DasMesh → Model Fusion).

Although the method of 4D model fusion is relative complicated, all the steps of it are integrated into the 3D model post-processing software DasMesh (Link) and the 3D model viewer software DasViewer(Link). We noted the menu location that provides the corresponding function at the end of each step, and the right-arrow indicates access to the sub-menu or button.

Evaluation metrics

It is a necessary scientific step that objectively and quantitatively evaluates the 3D model quality. Practically, we combine spatial precision, geometric refinement, and texture resolution to provide a comprehensive evaluation of 3D model quality.

Spatial precision. The spatial precision is a common metric in geomatics and photogrammetry. When deploying a multi-level control network, identical methods of setting up GCPs are used to deploy and survey a few of the checkpoints. The form of checkpoints is fully the same as the GCPs of the same level, but they are not involved in the ATS-control procedure. After obtaining the 3D model, we can calculate the planimetric and elevation errors through RMSE (root mean squared error) between the surveyed coordinates of checkpoints and their corresponding model coordinates.

In the case of a 3D model covering an area with a total of n_1 checkpoints, given the ith checkpoint with surveyed coordinates $O_{si}(X_{si}, Y_{si}, Z_{si})$ and model coordinates $O_{mi}(X_{mi}, Y_{mi}, Z_{mi})$, then the planimetric precision E_p and

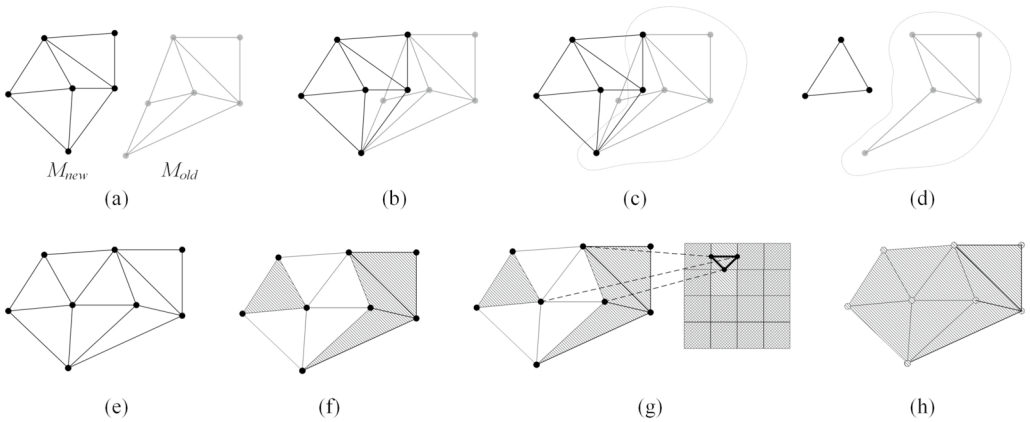

Fig. 5 The process of fusing 3D models. **a**, **b** Show the alignment of M_{new} and M_{old} through parameter transformation. **c** Shows the process of specifying the update range. **d** Shows shows cutting the patching through update range. **e** Shows the process of topological re-connection. **f** Shows that some texture errors have occurred. **g**, **h** Show the process and result of texture re-mapping

the elevation precision E_e of the 3D model is calculated as:

$$\begin{cases} E_p = \frac{1}{n_1}\sum_{i=1}^{n_1}\sqrt{(X_{si}-X_{mi})^2+(Y_{si}-Y_{mi})^2} \\ E_e = \frac{1}{n_1}\sum_{i=1}^{n_1}\sqrt{(Z_{si}-Z_{mi})^2} \end{cases} \quad (1)$$

In practice, we load the 3D model to DasViewer and then import the surveyed coordinates of the checkpoints. Thus, we can use the precision inspection function to complete the abovementioned operations.

Geometric refinement. The geometry of the 3D model is represented by the Delaunay triangular mesh formed by connecting 3D vertices. As we know, the more pixel points are used to represent an object, the photograph is clearer and finer. In the same way, the more triangular vertices are used to represent the same object, the 3D model is finer and richer in geometric detail. Therefore, in the same spatial extent, the more vertices, the finer the geometric structure. Since an edge of any triangle necessarily connects two vertices, and the edge lengths represent the actual distances between the two vertices in real-world coordinates, the edge length is an ideal measure for considering both the spatial extent and the number of vertices. We evaluate the geometric refinement of a 3D model by counting the average edge lengths of all triangles.

Given that the 3D model contains n_2 edges of a triangle, the ith edge connects vertices $V_{1i}(X_{1i}, Y_{1i}, Z_{1i})$ and $V_{2i}(X_{2i}, Y_{2i}, Z_{2i})$, then the geometric refinement R_g of the 3D model is calculated as:

$$R_g = \frac{1}{n_2}\sum_{i=1}^{n_2}\sqrt{(X_{1i}-X_{2i})^2+(Y_{1i}-Y_{2i})^2+(Z_{1i}-Z_{2i})^2} \quad (2)$$

In practice, we programmed the geometric refinement calculation of 3D models. We will soon develop a free and handy tool in DasViewer to provide this function.

Texture resolution. The same as images, 3D models also differ in clarity. However, unlike images that can be quantitatively evaluated for clarity with resolution, there is no method to measure the clarity of a 3D model yet.

Pixel density in units of *PPI* (Pixels Per Inch) is a commonly used metric for evaluating image clarity. Since the 3D model is rendered as a 2D image for display on the screen, we expect to evaluate the resolution of 3D models using *PPI* as image. To make it easy to grasp and generalize in 3D models, we propose the *PPMM* by replacing inches with the more commonly used length unit of millimeters (*MM*). A feasible way to measure the *PPMM* of a 3D model is as follows:

(1) Prepare the OBJ format file of the 3D model to be evaluated, which normally consists of one model file (.obj), one material library file (.mtl), and several texture image files (.png or .jpg).
(2) Open one of the texture images with image processing software. Randomly select a texture block and draw a straight line T_i within it, record the pixel number N_i of T_i, and save the changed image.
(3) Open the 3D model with a 3D viewer, find T_i, and measure its length, recording the length value in inches as L_i.
(4) The texture resolution R_i at the location of T_i is calculated as the ratio of N_i to L_i. Randomly repeated n_3 times, calculating the average value R_t of all the R_i, then R_t represent the texture resolution of the 3D model (Eq. 3).

$$R_t = \frac{1}{n_3}\sum_{i=1}^{n_3}\frac{N_i}{L_i} \quad (3)$$

In practice, we use DasMesh (Step 1), Windows Paint (Step 2), DasViewer (Step 3), and Microsoft Excel (Step 4) to achieve the above-mentioned operations. We will soon develop a free and handy tool in DasViewer to provide the functions of Step 2, Step 3 and Step 4.

Normally, the geometric refinement and texture resolution are relatively uniform in a 3D model, and 3D models are often divided into multiple tiles uniformly to alleviate the memory consumption of the computer. Therefore, we can randomly select one or more tiles to calculate geometric refinement and texture resolution.

Treatment of unqualified 3D model. In case the evaluation results indicate that the spatial accuracy is not qualified, it will be necessary to re-run the modeling program from ATS-control.

In case the evaluation results indicate that the geometric refinement and/or the texture resolution is not qualified, it will be necessary to identify the local area of poor quality, and then conduct complementary data collection for this area. Combining the original data with complementary data and then re-running the modeling program will be effective in improving the quality. This method of *Obtaining models—Evaluating quality—Collecting complementary data* is the most effective means to ensure that there are no omissions in data collection.

Results

We practice and verify the workflow and methods by dynamically documenting the excavation of the #3 fossil of hominin cranium from *Yunxian*. This section shows the major results.

Fig. 6 The appearance of GCPs at Level 1. **a**, **b** Show two different GCPs at Level 1 and scenarios using RTK to survey their geographic coordinates

Multi-level control network

In the excavation of the #3 fossil of hominin cranium from *Yunxian*, we deploy the multi-level control network as follows:

(1) Level 1: Painting L-shaped GCPs on the hardened road surface and surveying the geographic coordinates with RTK (Fig. 6).
(2) Level 2: Using survey nails to set up GCPs and surveying its geographic coordinates with RTK (Fig. 7).
(3) Level 3: Using marker board to set up GCPS and surveying its geographic coordinates with ETS from GCPs of L2 (Fig. 8).
(4) Level 4: Using mini label marked with *L* to set up GCPs and surveying its geographic coordinates with ETS from GCPs of L3 (Fig. 9).

Figure 10 illustrates the distribution of the GCPs in the Level 1 and Level 2 control networks. Figure 11a illustrates the introduction of the Level 3 control network from the Level 2 control network, and Fig. 11b illustrates the distribution of the GCPs in the Level 3 control network. Figure 12 illustrates a periodic Level 4 control network.

Under the standardized operation procedure, the error of the multi-level control network is the systematic error of RTK and ETS. If the measurements of the GCPs depend on the coordinates of the higher-level GCPs, the error will be accumulated. Table 2 shows the precision of the multi-level control network.

Data collection

At the *Yunxian Man* site, we conducted 1 data collection for the geographical environment and the archaeological

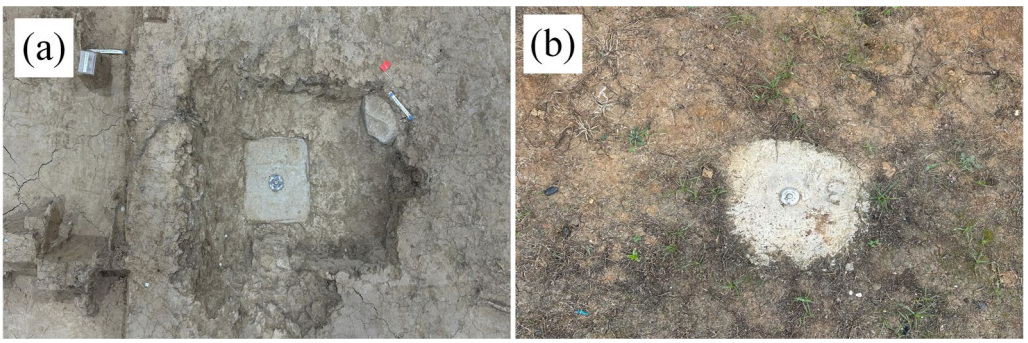

Fig. 7 The appearance of GCPs at Level 2. **a**, **b** Show two different GCPs at Level 2

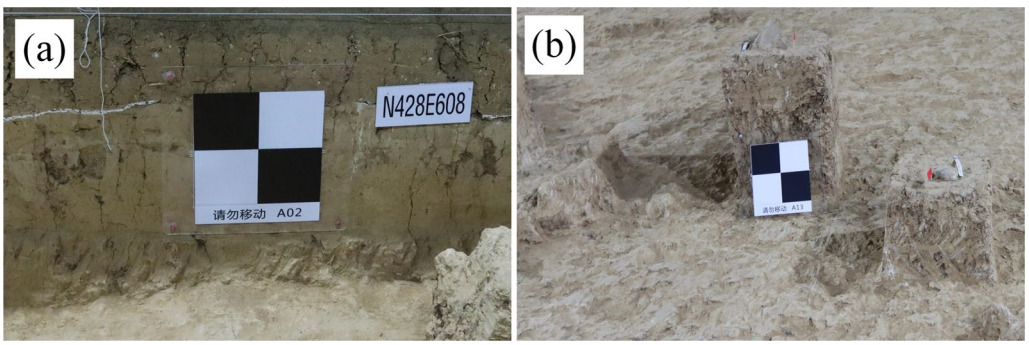

Fig. 8 The appearance of GCPs at Level 3. **a**, **b** Show two different GCPs at Level 3

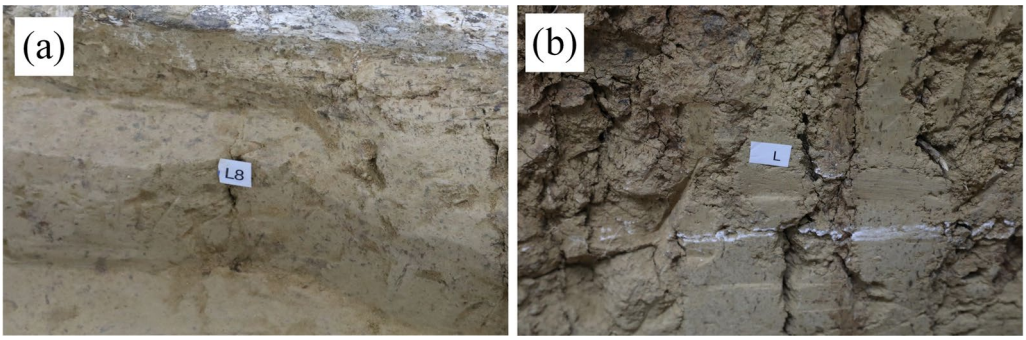

Fig. 9 The appearance of GCPs at Level 4. **a**, **b** Show two different GCPs at Level 4

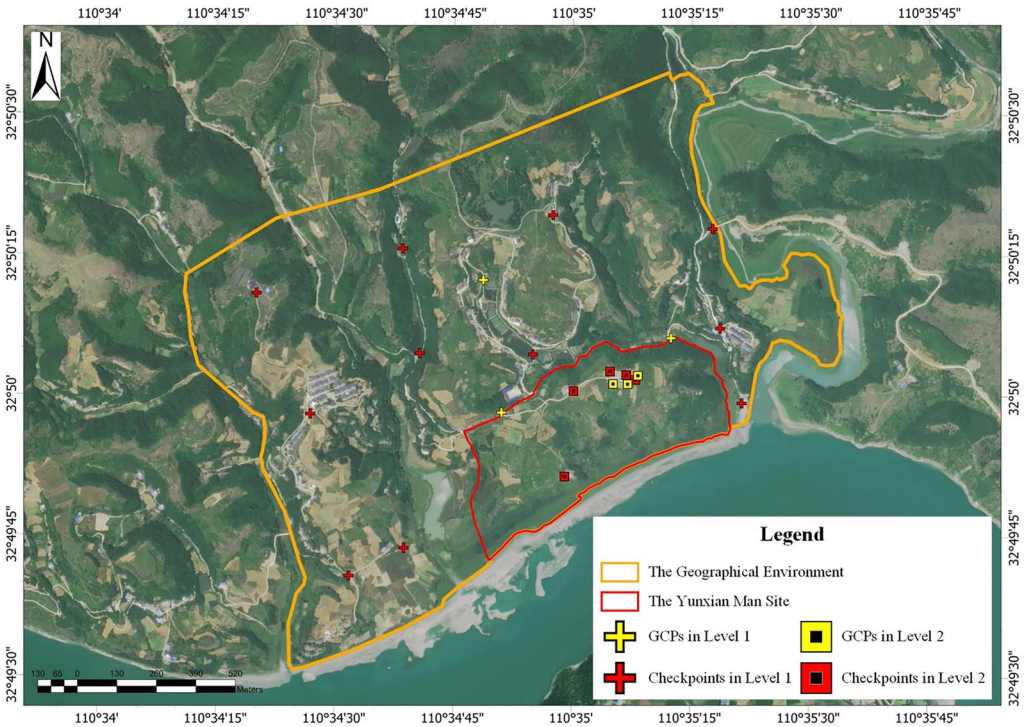

Fig. 10 The distribution of GCPs in Level 1 and Level 2. GCPs in Level 1 were relatively homogeneously distributed, and GCPs in Level 2 were appropriately clustered to the excavation areas

site because they were in a long-term stable state. During the excavation, we performed 6 data collections for the *Excavation Area B* and 14 data collections for the cultural remains.

Table 3 shows the Details of the data collection. The *Area* refers to the area of the effective coverage of the data. The *Frequency* refers to the times of data collection since the initiation of the current excavation in 2021. The *Resolution* refers to the spatial resolution, which is the most essential metric to describe the data quality.

The spatial resolution of the point cloud equals to the geometric refinement described in "Evaluation metrics" section. The spatial resolution of an image means the actual size of the object represented in one pixel. Due to terrain relief, image tilt, and many other reasons, the spatial resolutions are not uniform and constant within the same data. Therefore, we estimated the spatial resolution and presented their orders of magnitude in Table 3.

Cross-scale data fusion 3D modeling

Before the excavation, we conducted a geological survey of the archaeological site and the geographic environment through aerial photogrammetry. Due to the difference in area and importance, we adopted different flight

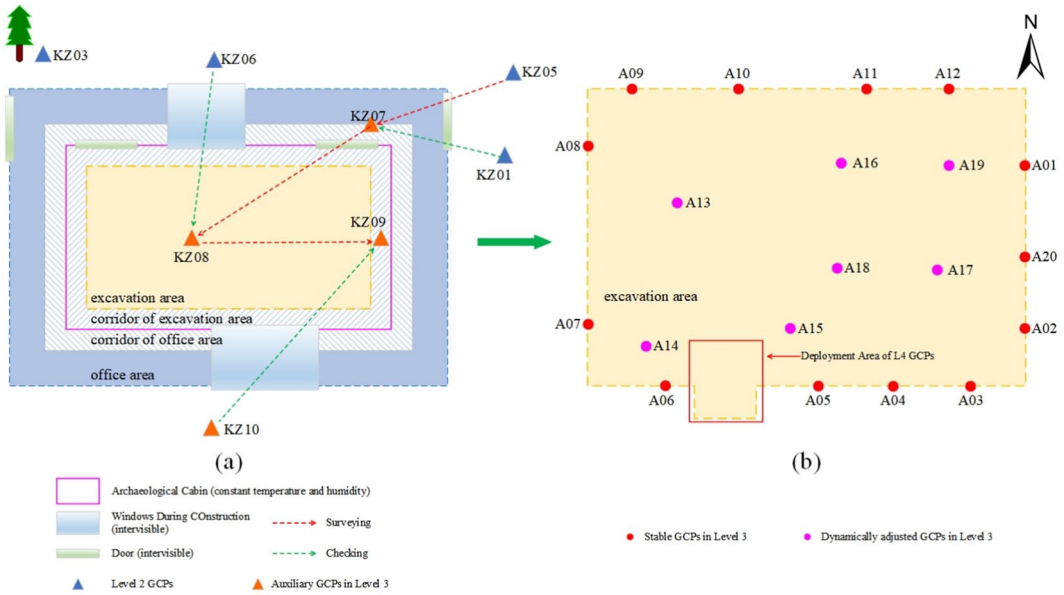

Fig. 11 Deploying the Level 3 control network based on the Level 2. **a** Shows that due to the absence of CORS signals, several GCPs in Level 3 were surveyed using ETS to set up stations on the GCPs in Level 2. Each of them is required once surveying and once checking to ensure the accuracy of the geographic coordinates. Then, KZ08 and KZ09 with known geographic coordinates can be used to survey and check the remaining GCPs in Level 3. **b** Shows that GCPs in Level 3 are relatively uniformly distributed; some of them are stable, and others are dynamically adjusted

Fig. 12 The periodic Level 4 control network. The GCPs in Level 4 are relatively uniformly distributed; some are stable, and others are dynamically adjusted. The geographic coordinates of the GCPs in Level 4 were surveyed by ETS at stations set up on the GCPs in Level 3

altitudes to improve the efficiency of data collection and optimize the cost of data processing. The flight altitude was 240 m for the geographic environment and 177 m for the archaeological site. For the *Excavation Area C*, we also used close-range photogrammetry to obtain more detailed data. Due to the large differences in the flight altitudes (or object distance) and camera parameters, we obtained data with different scales and resolutions. In this case, it is more difficult to obtain a unified 3D model using common methods. Thanks to the multi-level control network, we make these cross-scale data under an actual and unified coordinate framework, and then we use the method of cross-scale data fusion 3D modeling provided by GET3D to get a unified 3D model.

As a unified 3D model, it enables us to view and analyze the geographic environment, archaeological site, and excavation area just by mouse wheel zoom—without requiring us to switch to different 3D models. Figure 13 shows the 3D model of the *Yunxian Man* site and its geographical environment. In Fig. 14, the green lines of tile bounding indicate that it is a 3D model rather than a photograph, then sub-figure (a) shows that the 3D models of the geographic environment (outside the pink box) and the archaeological site (inside the pink box) achieve perfect fusion, sub-figure (b) shows that the 3D models of the archaeological site (outside the pink box) and the *Excavation Area C* (inside the pink box) achieve perfect fusion.

Multi-source data fusion 3D modeling

In the excavation of the #3 fossil of hominin cranium from *Yunxian*, we documented each transient but

Table 2 The precision of the multi-level control network

	GCP numbers	Survey method	Source of error	Precision (m) [a]	
				Planimetric↑	Elevation↓
Level 1	11	RTK	Systematic error of RTK	0.025	0.030
Level 2	4	RTK	Systematic error of RTK	0.025	0.030
Level 3	18–26	ETS based Level 2	Error of Level 2 + systematic error of ETS	0.030	0.035
Level 4	9–30	ETS based Level 3	Error of Level 3 + systematic error of ETS	0.035	0.040

[a] ↓ indicates that smaller values are more desirable, and ↑ indicates that larger values are more desirable. The same is true for the other tables in this paper

Table 3 Details of the data collection

	Area (m^2)	Frequency	Collection method	Data type	Resolution (m) ↓	Flight altitude (m)
Geographical environment	3.81×10^6	1	Aerial photogrammetry	Image	0.0300	240
Archaeological site	0.33×10^6	1	Aerial photogrammetry	Image	0.0200	177
Excavation area	208.52	6	Close-range photogrammetry	Image	0.0100	N/A
			Terrestrial laser scanning	Point cloud	0.0050	
Cultural remains	4.21	14	Close-range photogrammetry	Image	0.0005	N/A
			Portable laser scanning	point cloud	0.0002	

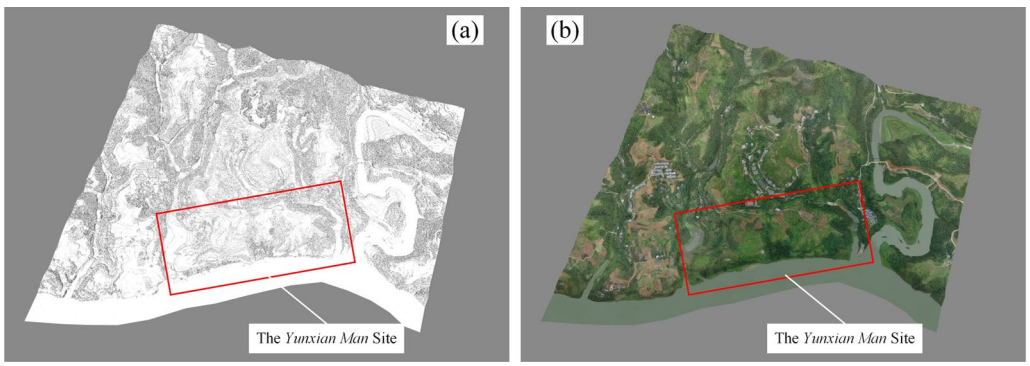

Fig. 13 The 3D model of the *Yunxian Man* site and its geographical environment. **a** Shows the high-precision geometric model. **b** Shows the high-realistic textured model

significant state of the *Excavation Area B* and the cultural remains using both photogrammetry and LiDAR scanning. After each data collection, we use GET3D to fuse photogrammetric images and laser point clouds to obtain high-precision and high-realistic 3D models.

Figure 15 shows a point cloud acquired by the terrestrial laser scanner at one station. We can see that occlusion and other reasons result in significant data deficiencies (i.e., voids), and the laser-scanned data are naturally absent of texture images. In practice, we can try to fill in these voids using multi-station scanning, but it is difficult to eliminate them completely as shade is ubiquitous. Figures 16 and 17 shows that using multi-source data fusion, a geometrically complete and highly realistic textured 3D model was obtained.

Fast cloud-based 3D modeling

In the excavation of the #3 fossil of hominin cranium from *Yunxian*, we conducted 6 data collections using close-range photogrammetry for the *Excavation Area B* (Table 3). Since it is not possible to fly UAVs in the cramped indoor area, these close-range photogrammetry can only be taken by manual photography. The *Excavation Area B* is over 200 m^2; it is too large to prevent omissions for manual photography. To engage the method of *Obtaining models—Evaluating quality—Collecting*

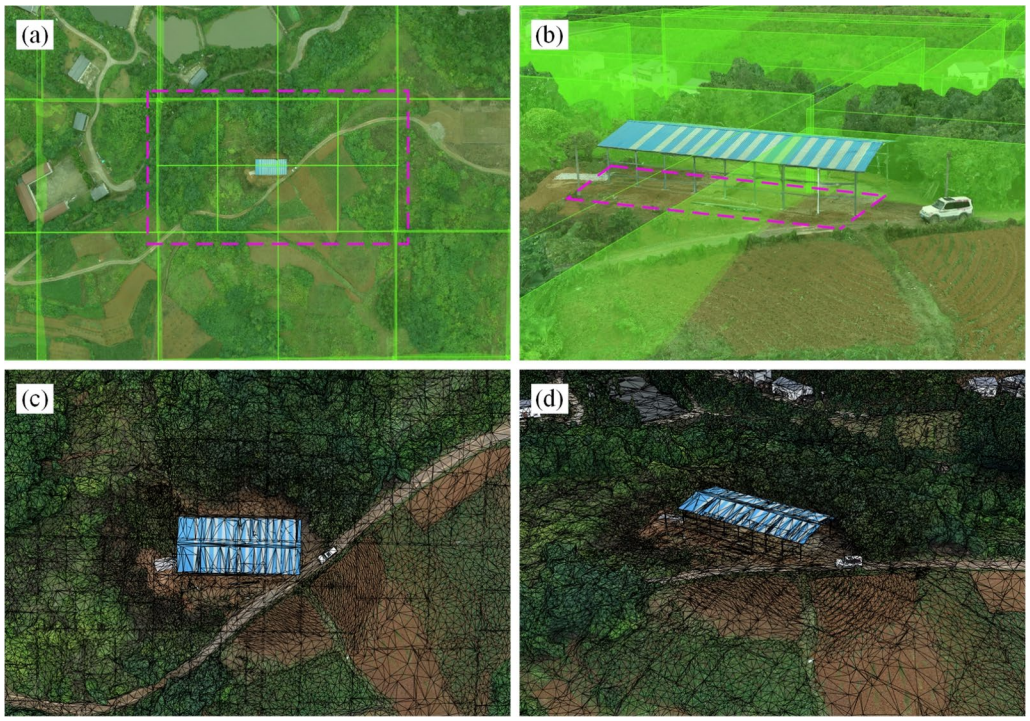

Fig. 14 Cross-scale models integrated into a unified framework. **a** That the 3D models of the geographic environment (outside the pink box) and the archaeological site (inside the pink box) achieve perfect fusion. **b** shows that the 3D models of the archaeological site (outside the pink box) and the *Excavation Area C* (inside the pink box) achieve perfect fusion. Through the wireframe mode, **c**, **d** show that the 3D model has a higher geometric refinement in the area of the archaeological site

complementary data to prevent omissions, we used DasEarth to process all these close-range images and generated 3D models (Fig. 16).

In our experiment, the single GPU workstation is configured with an Intel Core CPU and a Nvidia RTX4090ti GPU. DasEarth called 1 Synology NAS and 3 workstations, the workstations were equally configured with an

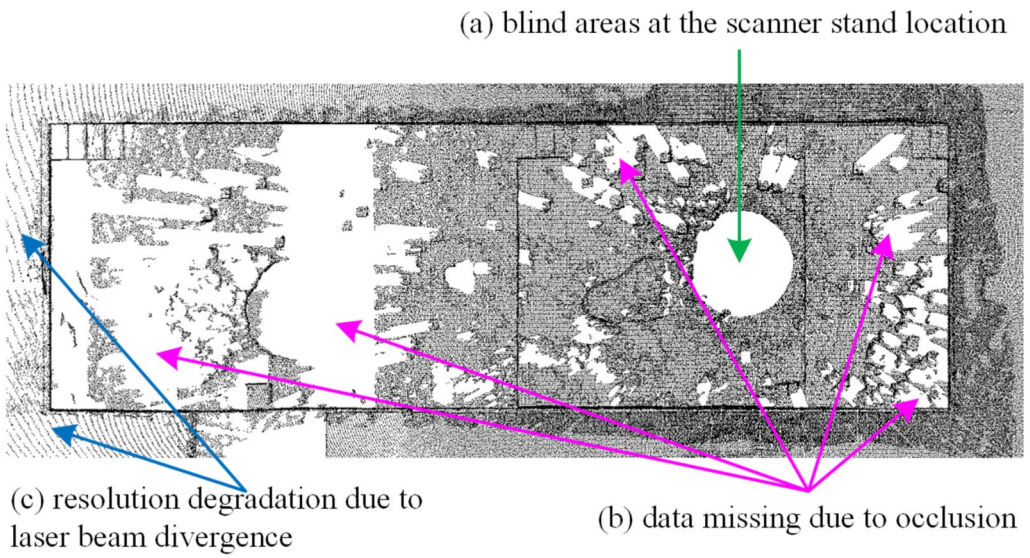

Fig. 15 A point cloud acquired by the terrestrial laser scanner at one station. It shows that occlusion and other reasons result in significant data deficiencies (i.e., voids), and the laser-scanned data are naturally absent of texture images. **a** Shows a circle void caused by blind areas at the scanner stand location. **b** Shows missing data in the radial distribution caused by occlusion. **c** Shows resolution degradation due to laser beam divergence

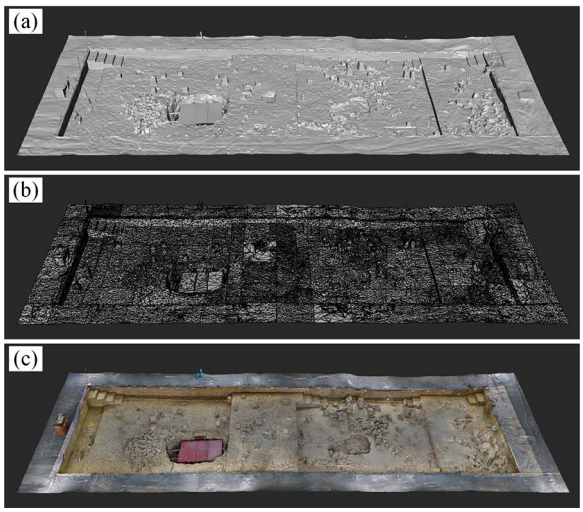

Fig. 16 The 3D model of the *Excavation Area B* at the *Yunxian Man* site. **a** Shows the high-precision geometric model. **b** Shows the wireframe model. **c** Shows the high-realistic textured model

Intel Core CPU and a Nvidia RTX4090ti GPU. Thanks to the efficiency of cloud modeling, we don't have to go through the dreaded long wait in the close-range photogrammetry for the *Excavation Area B*. We enumerate the runtime taken for each modeling with DasEarth in Table 4. For a single GPU workstation, we tested the runtime using the 6th modeling data (bold font in Table 4) and estimated the runtime for the other five modeling data (regular font in Table 4) based on an approximate linear relationship between the number of photos and the runtime.

Obviously, DasEarth is faster than a single GPU workstation. Moreover, DasEarth doesn't need a powerful and expensive GPU workstation; it just needs a mediocre laptop with Internet access or even a smartphone to accomplish the task.

4D model fusion

Archaeologists identified the integrity and significance of the #3 fossil of hominin cranium from *Yunxian* when it was just revealed. Then, a fossil excavation sub-area was defined by extending the location of the fossil outwards to four trenches (the pink rectangle in Fig. 18a). The works for the fossil excavation sub-area were meticulous and resulted in a more frequent requirement for digital documentation. As a result, a total of 14 data collections were made from the time the fossil was exposed until it was fully excavated (*Cultural Remains* in Table 3).

We used the 4D model fusion method to fuse the 3D models of the fossil excavation sub-area with the entire excavation area. The fusion result is a set of 4D models (Fig. 18). Each temporal phase in the set is a complete model of the entire excavation area, which supports archaeologists performing stratigraphic research and spatial analyses for the cultural remains. In sub-figure (a),

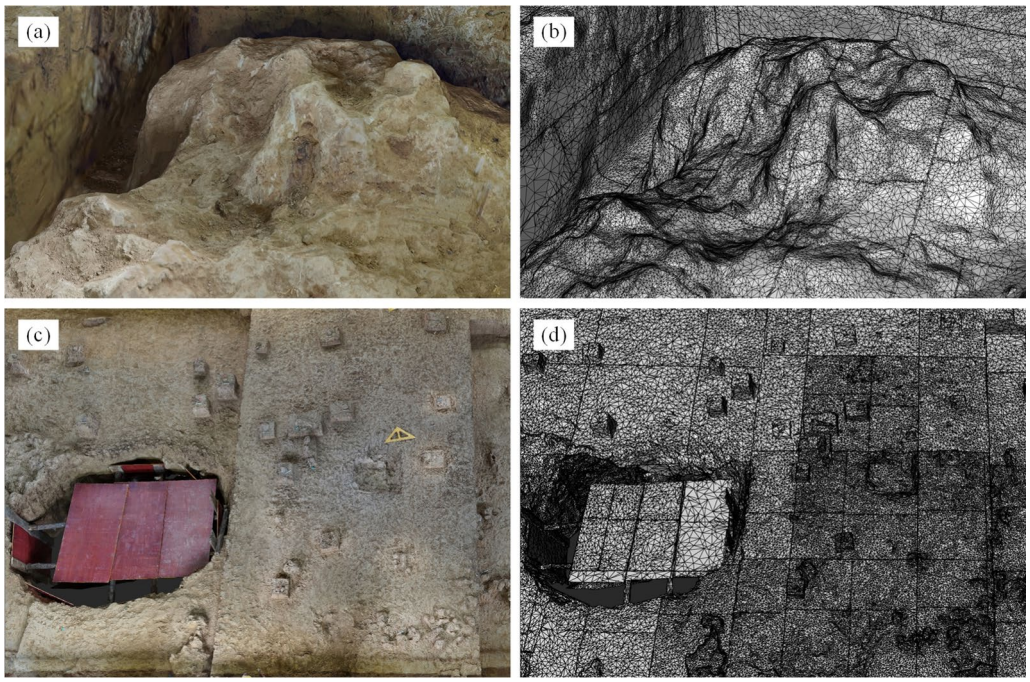

Fig. 17 Two partial zoom-in views of the 3D model of the *Excavation Area B* at the *Yunxian Man* site. **a**, **b** Show that the 3D model has a high geometric quality. **c**, **d** Show that the 3D model has different geometric refinement in different regions

Table 4 The number of images and the modeling times used for each update

	01	02	03	04	05	06
Number of images	13,661	15,098	12,405	18,933	20,157	24,710
Runtime of DasEarth (*h* : *m*)	11:30	12:11	10:06	16:38	19:43	22:16
Runtime of a single GPU Workstation (*h* : *m*)	40:37	44:54	36:54	56:18	59:57	**73:31**

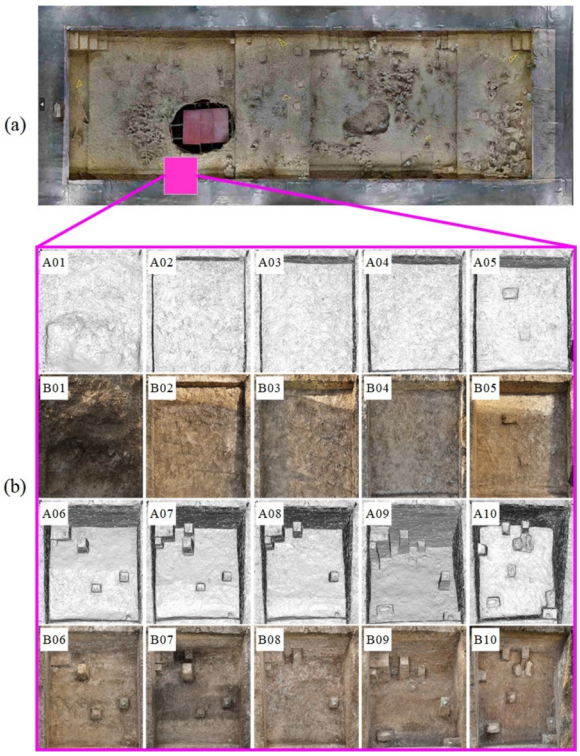

Fig. 18 A set of 4D models for the *Excavation Area B*. **a** Marks the fossil excavation sub-area in the *Excavation Area B*. **b** Shows the 4D models of the fossil excavation sub-area. More details will be updated on the project homepage (https://wyniu.github.io/DDAE/) in the future

the pink rectangles mark the update area. In sub-figure (b), multiple 3D models of the update area are shown by time; the first row shows the geometric model, and the second row shows the 3D model with texture.

Data quality

According to the evaluation metrics in "Evaluation metrics" section, we evaluated the 3D model quality of the excavation of the #3 fossil of hominin cranium from *Yunxian*. Table 5 presents all the evaluation results.

Discussion

Multi-level control network

(1) In our practice, we constructed 4D models for the excavation of the #3 fossil of hominin cranium from *Yunxian*. Thanks to the multi-level control network, the documented 3D models all carry actual geographic coordinates. It proves that the multi-level control network is capable of placing cross-scale archaeological objects in an actual and unified coordinate framework.

(2) In our proposed multi-level control network, the GCPs in Level 1 and Level 2 are relatively fixed, while the GCPs in Level 3 and Level 4 could change dynamically. The stabilized GCPs ensure the accuracy of the overall multi-level control network. The flexible GCPs enable the multi-level control network to continuously support the dynamically documenting archaeological excavations.

Cross-scale data fusion 3D modeling

(1) From the practice of fusing the data of the geographic environment, archaeological site, and excavation area together to construct a unified 3D model in "Cross-scale data fusion 3D modeling" section, we can conclude that (a) aerial photogrammetry enables fast data collection for large areas; (b) aerial photogrammetry with reduced altitude and close-range photogrammetry enables meticulous data collection to obtain adequate details; (c) together with multi-level control network, the method of cross-scale data fusion 3D modeling enables fuse cross-scale data to construct a unified 3D model.

(2) From a practical perspective, the method of cross-scale data fusion 3D modeling allows us to select data scales according to how many details are required—so as to optimize labor, time, and cost of data collection and processing.

Table 5 The evaluation of data quality

	ID[a]	Number of GCPs	E_p (m) ↓	E_e (m) ↓	R_g (mm) ↓	R_t (PPMM) ↑
Geographical environment	**01**	11	0.0242	0.0286	226.3109	0.02
Archaeological site	**01**	4	0.0181	0.0224	5.2725	3.06
Excavation area	**01**	18	0.0078	0.0086	0.1753	4.23
	02	20	0.0085	0.0152	0.1829	5.18
	03	20	0.0091	0.0112	0.2435	3.82
	04	21	0.0073	0.0146	0.1324	5.75
	05	19	0.0065	0.0139	0.0978	5.82
	06	21	0.0074	0.0127	0.0805	5.27
Cultural remains	**01**	15	0.0056	0.0061	0.0336	11.42
	02	14	0.0029	0.0082	0.0517	10.03
	03	13	0.0067	0.0079	0.1461	13.41
	04	14	0.0070	0.0064	0.0982	10.22
	05	15	0.0068	0.0038	0.1556	8.69
	06	16	0.0025	0.0081	0.0654	12.68
	07	15	0.0022	0.0053	0.0582	10.34
	08	15	0.0084	0.0035	0.0921	9.45
	09	18	0.0038	0.0094	0.0590	10.43
	10	19	0.0078	0.0088	0.1385	8.58
	11	19	0.0068	0.0055	0.1396	8.79
	12	22	0.0067	0.0062	0.0786	13.66
	13	23	0.0061	0.0059	0.1196	13.75
	14	22	0.0087	0.0071	0.0536	11.46

[a] The data with ID in bold font are available on our GitHub Repository (Link), which can be used to reproduce the evaluation process of R_g and R_t

Multi-source data fusion 3D modeling

It can be seen from "Multi-source data fusion 3D modeling" section that our technique and software achieve the fusion modeling of laser-scanned point clouds and photogrammetric images. We can pick some details to analyze the advantages of multi-source data fusion 3D modeling.

(1) Observing Fossil A in Fig. 19, the point cloud captured by the portable laser scanner is denser than the dense matched point cloud from photogrammetry. Naturally, the former also generates a more refined mesh than the latter. We fused the point clouds and then mapped the textures to obtain a 3D model with both high-precision geometry and highly realistic texture.
(2) Observing Fossil B in Fig. 19, the point cloud obtained by the terrestrial laser scanner produces some missing points due to viewpoint occlusion. Obviously, it produces meshes with voids. We fused the point clouds, and then the voids were repaired.

Eventually, the multi-source data fusion 3D modeling method enables us to obtain 3D models that preserve the dual advantages of LiDAR scanning and photogrammetry.

Fast cloud-based 3D modeling

(1) In the practice of "Fast cloud-based 3D modeling" section, when we use DasEarth to generate 3D models, we only require a mediocre laptop to upload data and stab GCPs, and the rest of the modeling work can be done entirely using the computility of the cloud. Therefore, the fast cloud-based 3D modeling technology helps us get rid of the dependence on local GPU workstations. As a result, archaeological teams do not need to finance purchasing GPU workstations, nor do they need to worry about the idle and wasteful use of expensive GPU workstations during times when they are not conducting field excavations.
(2) Analyzing the technical theory of fast cloud-based 3D modeling in "Fast cloud-based 3D modeling" section, multiple GPU laborers working in parallel will certainly be faster than a single GPU workstation locally. Table 4 also confirms this assumption. Therefore, the fast cloud-based 3D modeling technology could save a lot of time and also nicely solve

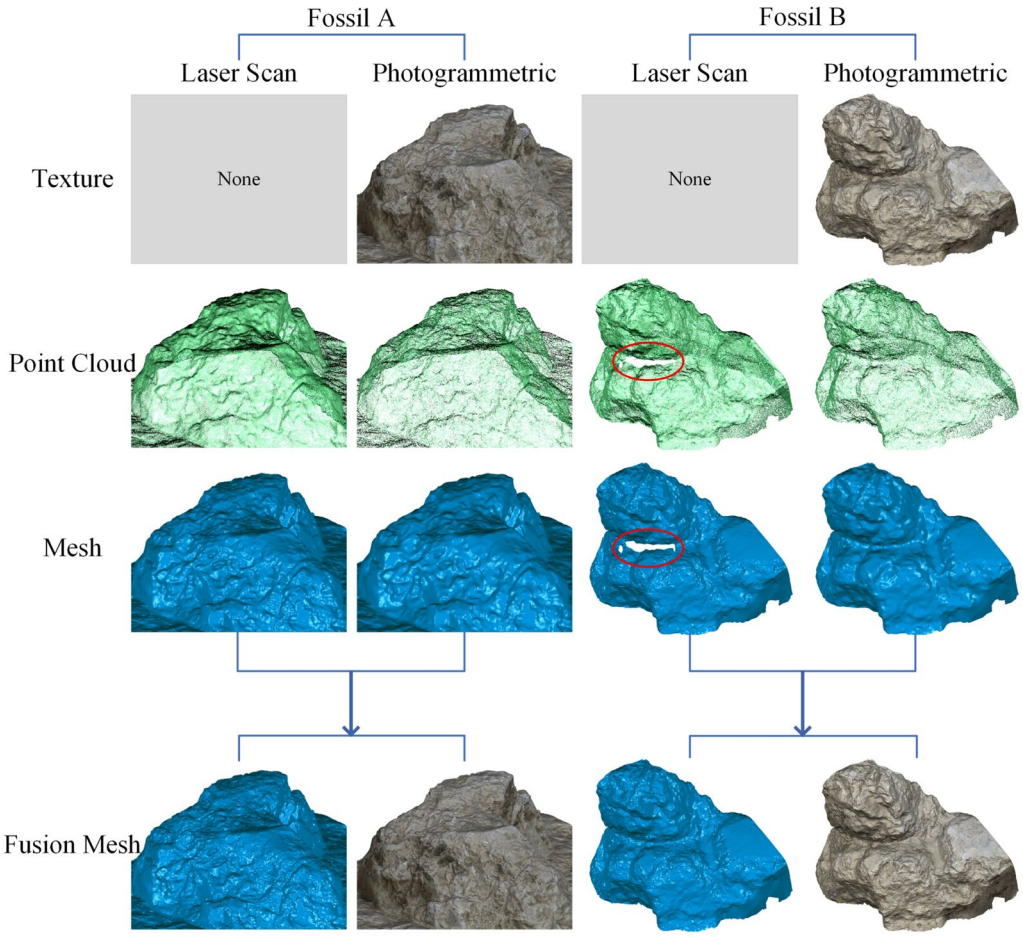

Fig. 19 Data fusion of photogrammetry and laser scanning. **a** Shows that the laser-scanned data of fossil A is not textured, while the photogrammetric data lacks sufficient geometrical refinement, and the fusion method yields a geometrically refined and textured 3D model. **b** Shows the laser-scanned data has a void caused by shading, and the fusion method fills it up

the problem of the phased surge of 3D modeling demand during archaeological excavations.

Overall, the fast cloud-based modeling technology offers multiple benefits, including financial savings, decreasing 3D modeling time, and making 3D modeling and sharing easier. This technology will be a true utility to facilitate dynamically documenting archaeological excavation, and a true platform to promote collaborative research through data sharing.

4D model fusion

As the practice of fusing the 3D models of the frequently changing excavation sub-area and the entire excavation area in "4D model fusion" section, the method of 4D model fusion enables us to document the dynamic process of change in the excavation area so as to support the sequential analysis along time.

To better analyze the value of the methods in this paper, we provide an additional case study of the *Zhengjiahu* Cemetery [34] in the "Appendix". To fulfill the requirement of comparatively analyzing the three tombs in the additional case study, we need to simultaneously present them in their just-opened state. However, the just-opened states of the three tombs were separated by several months. Thanks to the 4D model fusion method, we fused 3D models of the three tombs in their just-opened state into a unified 3D model. Therefore, the 4D model fusion method enables us to synthesize transient states of several excavation sub-areas into virtual scenes so as to support comparative analysis across time.

From a practical perspective, the method of 4D model fusion solves much tedious and time-consuming 3D modeling work by allowing us to simply focus on the sub-area that is being excavated—Otherwise, to get a complete model, we would have to conduct a data collection

and modeling of the *excavation area B* of 200 m^2 once whenever the fossil excavation sub-area of 4 m^2 changes.

Data quality

The planimetric precision E_p and the elevation precision E_e in Table 5 are commonly better than 0.03 m, even may be better than 0.01 m, and reach the millimeter level. Such evaluation results indicate that the 3D models carry geographical coordinates with ideal spatial accuracy. Moreover, since the algorithms of 3D measurement are based on geographic coordinates, the ideal spatial accuracy means we can perform reliable measurements for position, distance, area, and volume on these 3D models.

The geometric refinement R_g and texture resolution R_t in Table 5 are gradually enhanced from geographical environment to cultural remains. Indeed, our data collection is progressively finer from large to small scale. It indicates that our proposed geometric refinement and texture resolution are effective measures for the data quality.

Moreover, the data in Table 5 show that our methods enable high-precision modeling with geometric refinement reaching the sub-millimeter level and texture resolution of more than 10 PPMM.

Conclusions

Technological advancements promoted greater demands on using 3D modeling techniques to document archaeological excavations than ever before. The concept of documenting various momentary states for an ongoing archaeological excavation using 4D models can be formulated as dynamically documenting. Due to the practical difficulties of implementing dynamically documenting, we proposed a complete workflow and pursued several new methods, and practiced them in the excavation of the #3 fossil of hominin cranium from *Yunxian*. Our practical results show that:

(1) The multi-level control network enables all documented 3D models to be in an actual and unified coordinate framework.
(2) The proposed methods are capable of fusing data collected from different scales, equipment, and periods.
(3) The fast cloud-based modeling technology serves dual benefits. On the one hand, it aids archaeological teams in economically underdeveloped regions by alleviating their financial burdens, allowing them to engage in dynamically documenting without the concern of purchasing a sufficient number of GPU workstations. On the other hand, it offers all archaeologists and cultural heritage protectors a more efficient and user-friendly modeling service than several local GPU workstations.
(4) Through the comprehensive evaluation metrics, the documented 3D models can be precisely evaluated.

Our workflow and methods are capable to perform dynamically documenting archaeological excavation and obtain cross-scaled 4D models. Nevertheless, improvements still need to be incorporated into our technology. For example, images obtained from close-range photogrammetry inevitably contain some out-of-focus areas, which occasionally cause the texture of 3D models to be unclear. We will improve our technique by studying the optimal texture selection strategy.

In general, the proposed workflow and methods are proven effective and efficient since they eliminate tedious and time-consuming procedures. In addition, the entire process is easy to implement and generalize since the equipment and software we adopted are user-friendly. As a result, the workflow and methods enable us to obtain unified and 4D models with high-precision geometry and highly realistic texture. The 3D views enhance archaeologists' spatial perception of sites and relics, and the high-quality digital documentations support collaborative and long-term research based on data sharing. Therefore, the widespread adoption of the workflow and methods is promising to be conducive to archaeological fieldwork and in-depth research.

Appendix: Additional Case Study of the *Zhengjiahu* Cemetery

A brief introduction to the site. The *Zhengjiahu* Cemetery is located in Yunmeng County, Hubei Province, China, which is an important Warring States through Qin and Han cemetery. The *Excavation Area C* of the *Zhengjiahu* Cemetery was excavated in 2021. There, two Qin culture tombs, Nos. 274 and 234, yielded wooden *gu* slip with long texts and painted burial accouterments, respectively. The wooden *gu* slip, rarely in form and rich in content, is of significant value for the study of social history and ideology during the late Warring States. In addition, discovered painted burial accouterments fill a gap in current understandings of Qin and Han painting materials and types, providing crucial data for the study of Qin descendants' burial customs and rites, as well as religious ideology.

3D technology to document the excavation. We documented many transient but significant states of the *Excavation Area C* using the methods described in this paper. The significance of these digital documenting works lies in the fastest speed and highest resolution to capture and document the real-life spatial information

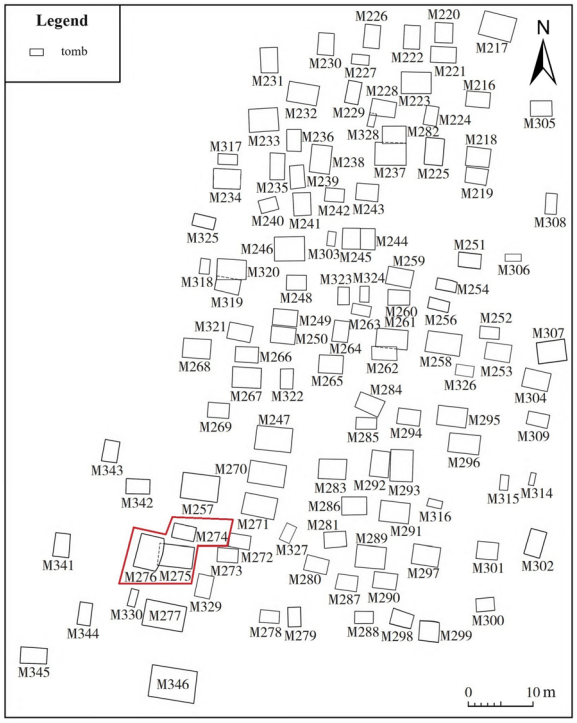

Fig. 20 The tombs ichnography in the *Excavation Area C* of the *Zhengjiahu* Cemetery. The red polygons label the objects studied in this paper, M274, M275, and M276

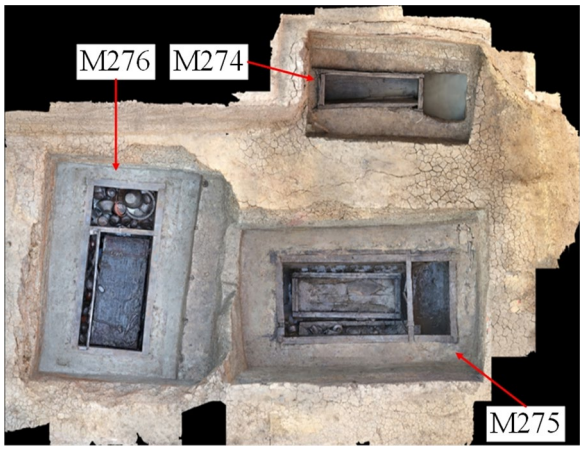

Fig. 21 The result of 4D model fusion. This figure shows the M274, M275, and M276 appearing to be realistically excavated together. However, the scene never really existed. Each tomb of them only existed for a few hours as they appear on the figure, and they were excavated several months apart from each other. Such a synthesized virtual scene is useful for archaeological research and spatial analysis

of the fragile organic archaeological remains, thus avoiding the omission of information that may be caused by the rapid oxidation and disappearance of cultural relics and the slow speed of manual documenting, and providing the possibility of future in-depth research, protection, and display.

The application of 4D model fusion. There are three adjacent tombs, M274, M275, and M276, in the *Zhengjiahu* Cemetery (Fig. 20). As the cultural relics in the tombs are extremely susceptible to oxidation and discoloration, the three tombs could only be excavated one after the other—so as to ensure that there were sufficient technicians available to protect the unearthed relics in time. Therefore, the coffins of the three tombs were opened at different times. After each coffin was opened, we used a UAV to conduct close-range photogrammetry as fast as possible, and then the archaeologists immediately transferred the relics. All of these tasks are usually accomplished within a few hours, and the appearance of the coffin just being opened is no longer in existence. However, archaeologists want to research the three tombs and analyze the relative orientation of their cultural relics as they were just being opened. Therefore, we employed the 4D model fusion method and fused the 3D models of three tombs constructed at different times into a unified 3D model. The fused 3D model is shown in Fig. 21, and it satisfied the needs of archaeologists in later studies.

This case demonstrates that the method of 4D model fusion enables us to fuse the spatial 3D models obtained at different excavation seasons and in different excavation areas into a complete, virtual 3D model, to obtain the complete information that can't be obtained from the excavations in different areas, and to discover the spatial features that can't be found from normal observations.

Acknowledgements
We are very grateful to the editors for their hard work to our manuscript!.

Author contributions
Wenyuan Niu wrote the paper and prepared the figures and tables. Yinghua Li and Xianfeng Huang supervised, reviewed, and revised the paper. Chengqiu Lu acted as the leader of the archaeological project. Qiushi Zou, Yinghua Li, and Xianfeng Huang provided technical guidance on dynamically documenting archaeological excavations. Wenyuan Niu, Xuan Wang, Hanyu Xiang, Cheng Wang, Qiushi Zou, Xuan Wei, and Wentai Lou accomplished the data collection. Wenyuan Niu and Dailong Huang were responsible for data processing. Dongqing Jiang, Fan Zhang, and Wenyuan Niu were responsible for the debugging of the software and code. Chengqiu Lu, Xing Gao, Yinghua Li, and Song Xing provided technical guidance on archaeological excavation. Song Xing, Xiaofeng Wan, Zhongyun Zhang, Jiayang Lu, Huanghao Yin, and Feng Wang accomplished the main works on archaeological excavation. Yunbing Luo completed the experiments and text writing in the "Appendix".

Funding
This work was supported by the Fundamental Research Funds for the Central Universities (No. 2042024kf0035).

Availability of data and materials
The original contributions are presented in the paper and "Appendix". Further reproduction guidance and the self-developed software are presented on the homepage of this project: https://wyniu.github.io/DDAE. Sample data

are presented in the Google Drive: https://drive.google.com/drive/folders/1q2z18tTiqOzJB4olOSLvL0ooDaApAhHm. The code used to reproduce the evaluation results are presented in the GitHub repository: https://github.com/WYNIU/DDAE_Compute_3D_Model_Refinement.

Declarations

Ethics approval and consent to participate

This paper does not contain any research involving humans or animals that have survived in the recent past. The *hominin cranium* or *animal fossils* mentioned in this paper means fossils from a million years ago and belong to archaeological research material that does not involve human or animal ethics, so this statement is not applicable.

Consent for publication

All authors of this paper and their affiliations have reviewed the paper and agreed to its public release.

Competing interests

The authors have no Conflict of interest as defined by Springer, or other interests that might be perceived to influence the results and/or discussion reported in this paper.

Author details

[1]Present Address: Archaeological Institute for Yangtze Civilization, Wuhan University, Bayi Road, Wuhan 430072, Hubei Province, China. [2]College of History and Philosophy, Tarim University, Junken Road, Alaer 843300, The Xinjiang Uygur Autonomous Region, China. [3]Hubei Provincial Institute of Cultural Relics and Archaeology, Donghu Road, Wuhan 430062, Hubei Province, China. [4]State Key Laboratory of Information Engineering in Surveying, Mapping and Remote Sensing, Wuhan University, Luoyu Road, Wuhan 430070, Hubei Province, China. [5]Institute of Vertebrate Paleontology and Paleoanthropology, Chinese Academy of Sciences, Xizhimenwai Street, Beijing 100044, Beijing, China. [6]School of History, Wuhan University, Bayi Road, Wuhan 430072, Hubei Province, China. [7]Intelligent Computing Laboratory for Cultural Heritage, Wuhan University, Bayi Road, Wuhan 430072, Hubei Province, China. [8]CNRS UMR 7041 ArScAn-AnTET, Université Paris X, Nanterre, France. [9]Daspatial Technology Co., LTD, Guanggu Road, Wuhan 430223, Hubei Province, China. [10]Henan Provincial Institute of Cultural Relics and Archaeology, Longhaibeisan Street, Zhengzhou 430072, Henan Province, China. [11]Xingshan Folklore Museum, Yichang 443799, Hubei Province, China.

Received: 27 March 2024 Accepted: 1 July 2024
Published online: 02 August 2024

References

1. Rüther H, Chazan M, Schroeder R, Neeser R, Held C, Walker SJ, Matmon A, Horwitz LK. Laser scanning for conservation and research of African cultural heritage sites: the case study of Wonderwerk Cave, South Africa. J Archaeol Sci. 2009;36(9):1847–56.
2. Tapete D, Casagli N, Luzi G, Fanti R, Gigli G, Leva D. Integrating radar and laser-based remote sensing techniques for monitoring structural deformation of archaeological monuments. J Archaeol Sci. 2013;40(1):176–89.
3. Doneus M, Neubauer W. 3d laser scanners on archaeological excavations. In: Proceedings of the XXth International Symposium CIPA, Torino, 2005. p. 226–231.
4. Wang S, Hu Q, Wang F, Ai M, Zhong R. A microtopographic feature analysis-based LiDAR data processing approach for the identification of Chu tombs. Remote Sens. 2017;9(9):880.
5. Gallo A, Muzzupappa M, Bruno F. 3d reconstruction of small sized objects from a sequence of multi-focused images. J Cult Herit. 2014;15(2):173–82.
6. Gong Y, Zhang F, Jia X, Huang X, Li D, Mao Z. Deep neural networks for quantitative damage evaluation of building losses using aerial oblique images: case study on the great wall (China). Remote Sens. 2021;13(7):1321.
7. Yang X, Grussenmeyer P, Koehl M, Macher H, Murtiyoso A, Landes T. Review of built heritage modelling: integration of HBIM and other information techniques. J Cult Herit. 2020;46:350–60.
8. Achille C, Adami A, Chiarini S, Cremonesi S, Fassi F, Fregonese L, Taffurelli L. UAV-based photogrammetry and integrated technologies for architectural applications-methodological strategies for the after-quake survey of vertical structures in Mantua (Italy). Sensors. 2015;15(7):15520–39.
9. Themistocleous K, Ioannides M, Agapiou A, Hadjimitsis DG. The methodology of documenting cultural heritage sites using photogrammetry, UAV, and 3D printing techniques: the case study of Asinou Church in Cyprus. In: Third International Conference on Remote Sensing and Geoinformation of the Environment (RSCy2015), 2015; vol. 9535. p. 312–318. SPIE.
10. Stek TD. Drones over Mediterranean landscapes. . The potential of small UAV's (drones) for site detection and heritage management in archaeological survey projects: A case study from Le Pianelle in the Tappino Valley, Molise (Italy). J Cult Herit. 2016;22:1066–71.
11. McCarthy J. Multi-image photogrammetry as a practical tool for cultural heritage survey and community engagement. J Archaeol Sci. 2014;43:175–85.
12. Aicardi I, Chiabrando F, Lingua AM, Noardo F. Recent trends in cultural heritage 3d survey: the photogrammetric computer vision approach. J Cult Herit. 2018;32:257–66.
13. Dellepiane M, Dell'Unto N, Callieri M, Lindgren S, Scopigno R. Archeological excavation monitoring using dense stereo matching techniques. J Cult Herit. 2013;14(3):201–10.
14. Campana S, Remondino F. Fast and detailed digital documentation of archaeological excavations and heritage artifacts. In: Layers of Perception—CAA 2007, 2008;36–42. Bonn: Dr. Rudolf Habelt GmbH
15. Doneus M, Verhoeven G, Fera M, Briese C, Kucera M, Neubauer W. From deposit to point cloud—a study of low-cost computer vision approaches for the straightforward documentation of archaeological excavations. Geoinf FCE CTU. 2011;6:81–8.
16. Korumaz M, Betti M, Conti A, Tucci G, Bartoli G, Bonora V, Korumaz AG, Fiorini L. An integrated terrestrial laser scanner (TLS), deviation analysis (DA) and finite element (FE) approach for health assessment of historical structures. A Minaret case study. Eng Struct. 2017;153:224–38.
17. Alshawabkeh Y, El-Khalili M, Almasri E, Bala'awi F, Al-Massarweh A. Heritage documentation using laser scanner and photogrammetry. The case study of Qasr Al-Abidit, Jordan. Dig Appl Archaeol Cult Herit. 2020;16:00133.
18. Şenol Hİ, Memduhoglu A, Ulukavak M. Multi instrumental documentation and 3d modelling of an archaeological site: a case study in Kizilkoyun Necropolis area. Dicle Üniversitesi Mühendislik Fakültesi Mühendislik Dergisi. 2020;11(3):1241–50.
19. Psarros D, Stamatopoulos MI, Anagnostopoulos C-N. Information technology and archaeological excavations: a brief overview. Sci Cult 2022;8(2):147–67.
20. De Reu J, De Smedt P, Herremans D, Van Meirvenne M, Laloo P, De Clercq W. On introducing an image-based 3d reconstruction method in archaeological excavation practice. J Archaeol Sci. 2014;41:251–62.
21. Galeazzi F. Towards the definition of best 3d practices in archaeology: sessing 3d documentation techniques for intra-site data recording. J Cult Herit. 2016;17:159–69.
22. Borg B, Dunn M, Ang A, Villis C. The application of state-of-the-art technologies to support artwork conservation: literature review. J Cult Herit. 2020;44:239–59.
23. Li T, Wang Z, Li W, Feng X, Hu K, Liu W. Survey and test excavation of fossil sites in Quyuanhekou, Yun county, Hubei Province. Jianghan Archaeol. 1991;2:1–14.
24. Lu C, Wan X, Xie S, Huang X, Liu Y, Xing S, Gao X. 2022 archaeological harvest from the site of the Xuetangliangzi Site (the Yunxian human site) in Hubei. Jianghan Archaeol. 2023;01:5–92.
25. Tianyuan L, Etler DA. New middle Pleistocene hominid crania from Yunxian in China. Nature. 1992;357(6377):404–7.
26. Pope GG. Craniofacial evidence for the origin of modern humans in China. Am J Phys Anthropol. 1992;35(S15):243–98.
27. Vialet A, Guipert G, Jianing H, Xiaobo F, Zune L, Youping W, Tianyuan L, Lumley M-A, Lumley H. Homo erectus from the Yunxian and Nankin Chinese sites: anthropological insights using 3D virtual imaging techniques. C R Palevol. 2010;9(6–7):331–9.
28. Yinyun Z. Fossil human crania from Yunxian: morphological comparison with Homo erectus crania from Zhoukoudian. Acta Anthropol Sin. 1995;14(01):1.

29. Chen T-M, Yang Q, Hu Y-Q, Bao W-B, Li T-Y. ESR dating of tooth enamel from Yunxian Homo erectus site, China. Quat Sci Rev. 1997;16(3–5):455–8.
30. Sun X, Li Y, Feng X, Lu C, Lu H, Yi S, Wang S, Wu S-Y. Pedostratigraphy of aeolian deposition near the Yunxian Man site on the Hanjiang River terraces, Yunxian Basin, central China. Quat Int. 2016;400:187–94.
31. Arun KS, Huang TS, Blostein SD. Least-squares fitting of two 3-d point sets. IEEE Trans Pattern Anal Mach Intell. 1987;5:698–700.
32. Besl PJ, McKay ND. A method for registration of 3-d shapes. IEEE Trans Pattern Anal Mach Intell. 1992;14(2):239–56.
33. Zhang Z. Iterative point matching for registration of free-form curves and surfaces. Int J Comput Vis. 1994;13(2):119–52.
34. Luo Y, Zhao J, Shi D, Zhang H, Li F, Sun J. A preliminary report on 2021 excavation of Zhengjiahu cemetery, Yunmeng County, Hubei Province. Archaeology. 2022;02:3–212.

Publisher's Note